Synthesis and Characterization of Novel Segmented Polyurethane/Clay Nanocomposite via Poly(ε-caprolactone)/Clay

T. K. CHEN, Y. I. TIEN, K. H. WEI

Department of Materials Science and Engineering, National Chiao Tung University, Hsinchu, Taiwan 30049, Republic of China

Received 17 August 1998; accepted 7 December 1998

ABSTRACT: A novel segmented polyurethane/clay (PU/clay) nanocomposite based on poly(caprolactone), diphenylmethane diisocyanate, butanediol, and poly(caprolactone)/clay prepolymer was synthesized as evidenced by FTIR and X-ray diffraction studies. Poly(caprolactone)/clay (PCL/clay) prepolymer was first synthesized in a nanocomposite form as confirmed by X-ray diffraction. X-ray diffraction study showed that PU/clay contained crystalline structure due to the presence of PCL/clay. In mechanical properties, about 1.4% PCL/clay in PU/clay resulted in a large increase in the elongation of PU/clay. However, when the amount of PCL/clay was 4.2%, the elongation of PU/clay was reduced drastically. This behavior indicated that PU/clay can be transformed from an elastomer to a thermoplastic material as the amount of PCL/clay in PU/clay increased. Additionally, the lap shear stress of PU/clay was at least three times that of neat PU as a result of the PCL/clay component. © 1999 John Wiley & Sons, Inc. J Polym Sci A: Polym Chem 37: 2225–2233, 1999

Keywords: nanocomposite; clay; segmented polyurethane; polycaprolactone; tensile properties

INTRODUCTION

Polymer composites were widely used in electronic and information products, consumer commodities, and the construction industry. In these polymer composites, inorganic materials were used to reinforce polymers with the idea of taking advantage of the high heat durability and the high mechanical strength of inorganics and the ease of processing polymers. Realistically, the interfacial incompatibility between inorganics and organic polymers existed owing to the difference in the nature of their individual intermolecular interaction forces and often caused failures in these inorganic/organic composites. This interfacial problem is the focus of various research activities. Moreover, the amount of inorganics used in these traditional polymer composites is usually more than 10% by weight for imparting the desired mechanical properties. When more than 10% of inorganics is added to the polymer, there are deteriorating properties associated with the composites, such as an increase in density and a loss of tenacity.

One approach to alleviate the interfacial and the tenacity problem in these polymer composites is to chemically bond the inorganics and polymers through the sol–gel method.[1–8] A series of inorganics–polymer hybrid composites were produced by the sol–gel method. The hybrid materials prepared by the sol–gel method suffered the drawback of large shrinkage during the removal of the solvent. The other approach is to uniformly disperse the inorganics in the polymer matrix in the

Correspondence to: K. H. Wei

Journal of Polymer Science: Part A: Polymer Chemistry, Vol. 37, 2225–2233 (1999)
 CCC 0887-624X/99/132225-09

nanometer scale to form inorganics/polymer nanocomposites.[9–12] This method can produce homogeneous inorganics/polymer composites in an efficient process without introducing the shrinkage as produced in the sol–gel method. Since the advent of the superior Nylon 6 montmorillonite nanocomposite developed by Toyota Motor Co.,[13–15] a large number of studies on polymer/clay nanocomposites were performed. Epoxy/clay,[16–18] polyimide/clay,[19–20] polyethylene oxide/clay,[21–22] polycaprolactone/clay[23] (PCL/clay), and polymethylmethacrylate/clay[24] were synthesized. On the other hand, elastomer/clay[25–27] nanocomposites were not sufficiently exploited. In this study we are interested in developing segmented polyurethane/clay (PU/clay) nanocomposites.

The structures and properties of thermoplastic segmented polyurethane (PU) had been studied by different research groups.[28–30] The linear structure of segmented PU is in the form of $(A - B)_n$. The soft segment B is formed from polyester or polyether macrogel of molecular weight between 1000 and 3000, and the hard segment is formed from 1,4-butanediol (1,4-BG) and diisocyanate. Phase separation occurred and formed microdomains in segmented PU. This phenomenon resulted from the relatively short length of hard segment chains and the mutual attraction of these hard segments by hydrogen bonding.

The objective of this study is to design a new segmented PU containing synthesized PCL/clay for a partial replacement of the 1,4-BG in the hard segment. A low molecular weight PCL/clay prepolymer was first synthesized in this study. The effect of PCL/clay content on the crystallization and mechanical properties of the synthesized segmented PU/clay was analyzed.

EXPERIMENTAL

Materials

ε-Caprolactone (99%, Lancaster), 4,4′-diphenyl methane diisocyanate (MDI; TCI), 1,4-BG (Tedia), polycaprolactone diol (M_n = 1000; CAPA214, Solvay), and dimethylformamide (DMF; Baker) were used as received.

Preparation of Organoclay

Source clay Swy-1 (Wyoming Na^+-montmorillonite) was obtained from the Clay Minerals Depository at the University of Missouri, Columbus, MO. A protonated amino acid of 12-aminolauric acid (TCI) was used as received. After screening Swy-1 Na^+-montmorillonite with a sieve of 325-mesh to remove impurities, a clay having a cationic exchange capacity of 76.4 M equiv/100 g was obtained. Screened montmorillonite of 10 g was gradually added to an already prepared solution of 12-aminolauric acid (2.16 g dissolved in 1000 mL of 0.01*N* HCl) at 60°C and vigorously stirred for 3 h. The treated montmorillonite was washed repeatedly with deionized water. The filtrate was titrated with 0.1*N* $AgNO_3$ until no further formation of AgCl precipitated to ensure the complete removal of chloride ions. The filter cake was then placed in a vacuum oven at 80°C for 12 h drying. The dried cake was ground and screened with a 325-mesh sieve to obtain the organoclay.

Synthesis of PCL/Clay Nanocomposites

ε-Caprolactone monomer was first dried with CaH_2, and then distilled under reduced pressure to remove moisture. Distilled monomer of 95 g and 5 g of organoclay were mixed in a three-neck flask and heated to 170°C. The mixtures were stirred for 3 h to complete the reaction. Next, the resultant product was dissolved with THF and then was filtered. The filtrate was precipitated in hexane, and after filtering, the filter cake was placed in a vacuum oven maintained at 80°C for 12 h to obtain PCL/clay nanocomposite.

Synthesis of PU/Clay Nanocomposite

The DMF solvent was distilled over CaH_2 under reduced pressure and stored in the presence of 4 Å molecular sieve to keep it dry. Segmented PUs were synthesized by a two-step process. A stoichiometric mixture of MDI, polycaprolactone diol, and DMF was placed in a 1000-mL glass reactor under stirring at 70°C for 2 h, followed by a reaction in solution with the chain extender, 1,4-BG for 30 min. Subsequently, PCL/clay nanocomposite was added to the mixture and the whole system was stirred for 30 min. The resulting PU/clay in DMF was poured into a flat mold of 2-mm thickness and set overnight. The PU/clay in DMF was placed in a vacuum oven at 80°C for 10 h drying.

Polymer Recovery

2 mL of toluene was added to 0.2 g of the synthesized PCL/clay while stirring for 2 h at room

temperature. After filtration, a clear PCL/clay solution was obtained. The clear PCL solution was then gradually stirred into 4 mL of 1% LiCL solution that was prepared by using equal volume ratio (v/v) of toluene and DMF. The finished mixture was placed at room temperature for 48 h to perform the reverse ion-exchange reaction. After the ion exchange, the solution was centrifuged at 5000 rpm for 5 min. The supernatant liquid after centrifuge was distilled under reduced pressure to remove the solvent; thus, the PCL polymer was obtained by reversed ion exchange on the silicate layer. In a similar manner, pure PU was recovered from PU/clay nanocomposites, except that the 1.0 wt % LiCL solution was prepared by using pure DMF.

Characterization

PCL/clay and PU/clay samples were scanned at a rate of 4°/min by Shimadzu XD-5 X-ray diffractometer (XRD; 30 kV, 10 mA) with copper target and Ni filter. For each interval of 0.01°, the diffracted X-ray intensity was recorded automatically. The differential scanning calorimetry (DSC) analyses of samples were carried out under N_2 atmosphere with model 2910 analyzer (Du Pont) at a heating rate of 20°C/min. The molecular weights of PCL/clay and PU/clay were determined by Waters 510 GPC with DMF as the solvent. The GPC measurements performed on polymer/clay and polymer recovered from polymer/clay nanocomposites using ion-exchange reaction. The calibration curves for GPC were obtained by using polystyrene and polyethylene glycol standards. Infrared spectroscopic experiments on PU/clay nanocomposites were performed with a Perkin–Elmer Spectrum 2000 Fourier transform infrared spectrometer. A 10% solution of the segmented PU nanocomposite in deuterated chloroform was prepared for ^{1}H-NMR analysis by using a Brucker AM-400 NMR spectrometer. The tensile strength tests were carried out with an Instron 4468 machine according to ASTM D412/75. Samples were cut to 33 × 6 × 1-mm size, and the crosshead speed was set at 500 mm/min. The lap strength tests were performed with Instron 4468 according to ASTM D1002 and crosshead speed was set at 1.3 mm/min. The samples for the lap strength test were adhered to pretreated aluminum plates. For each data point, five samples were tested and the average value was taken.

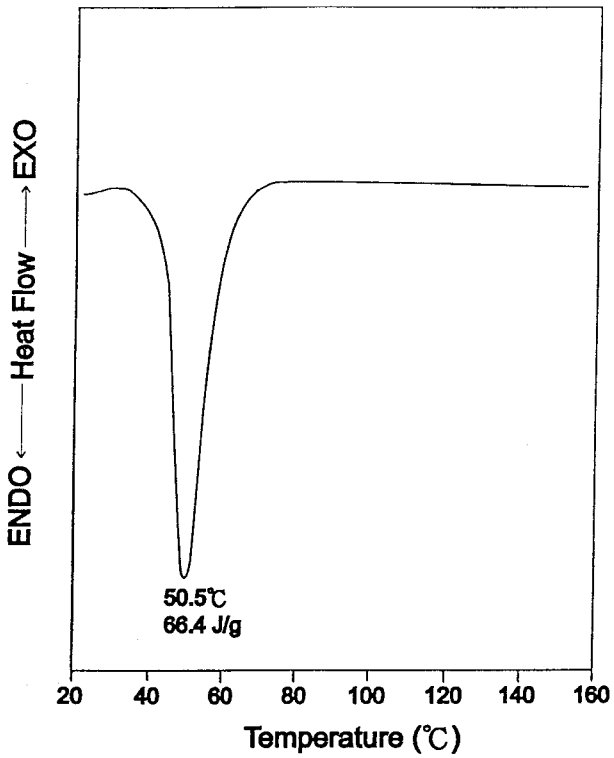

Figure 1. DSC curve of the PCL/5 wt % $[H_3N(CH_2)_{11}COOH]^+$–Mont.

RESULTS AND DISCUSSION

The DSC curve of synthesized PCL/clay was shown in Figure 1. In Figure 1, the melting temperature (T_m) of PCL/clay is 50.5°C, and PCL/clay possessed a large melting peak with a heat fusion of 66.4 J/g, revealing the existence of high crystallinity. After the polymer recovery process, the polymer chains of PCL and PU were released from the silicate layers, and pure PCL and PU were dissolved in DMF perfectly; thus, the number-averaged molecular weight (M_n) of PCL was 3440 as measured by GPC analysis and 3270 by the end-group analysis with H^1-NMR. Since the PCL chains were severed from silicate layers, the molecular weight of pure PCL determined from GPC and ^{1}H-NMR cannot be used to elucidate the branch number of PCL/clay. Therefore, the branch number of PCL/clay cannot be determined by this study, although in reality, a similar star polyamide/clay structure was found by Usuki et al.[31] The mechanism of ring-opening reaction during the synthesis of PCL and the resulted PCL/clay structure is displayed in Figure 2. In Figure 2, the ammonium cation in the organoclay initi-

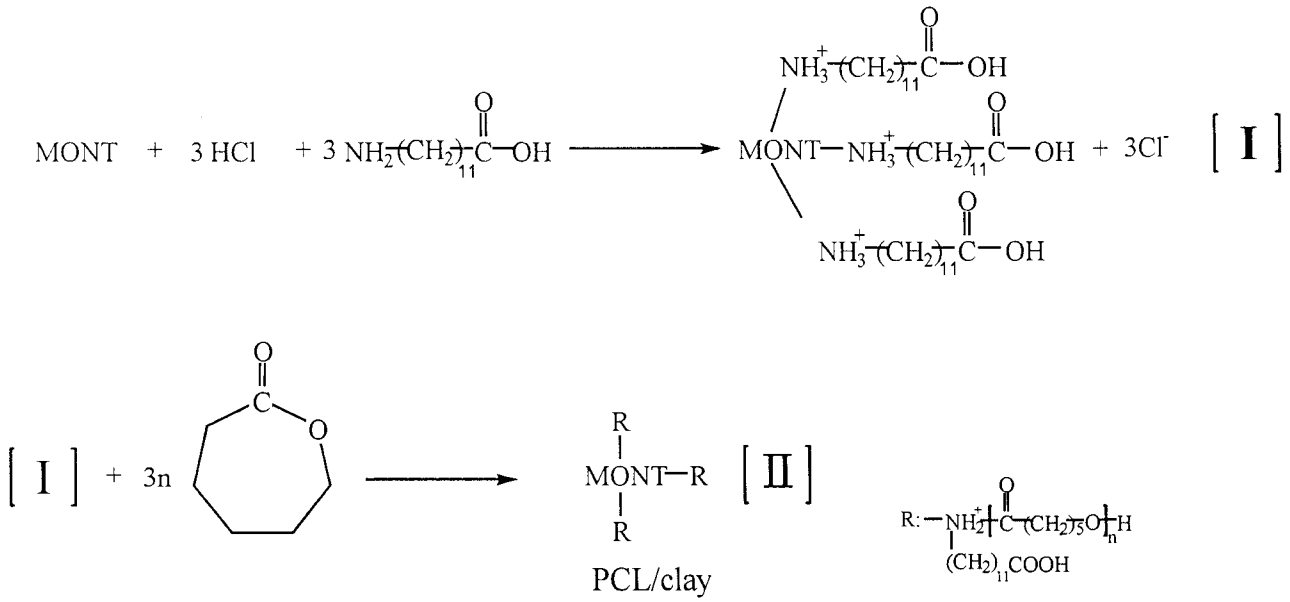

Figure 2. Synthesis of $[H_3N(CH_2)_{11}COOH]^+$–Mont and PCL/5 wt % $[H_3N(CH_2)_{11}COOH]^+$–Mont.

ated the ring opening of ε-caprolactone by attacking its carbonyl group, although in one article, by Messersmith[23] et al., it was mentioned that the carbonylic acid was the initiation group. This species continued to react with ε-caprolactone to form PCL/clay. The XRD patterns of synthesized PCL/clay, clay, and organoclay were shown in Figure 3. In Figure 3, the sharp reflections at $2\theta = 5.18°$, with a corresponding d spacing of 15.2Å, was caused by the stacked silicate layer structure in the organoclay. When PCL/clay was formed, the clay peak at $2\theta = 5.18°$ disappeared in the diffraction pattern of PCL/clay. This clearly indicated that an exfoliation of the silicate layer structure of organoclay in PCL occurred. The two strong peaks at $2\theta = 21.3°$ and 23.7° represented the induced crystalline structure of PCL[23] by the dispersed silicate layers. Thus, PCL/clay material is a nanocomposite material.

The chemical structure of synthesized PU and PU/clay nanocomposites are shown in Figure 4. The codes, the compositions, and the actual content of synthesized PU/clay nanocomposites formed by a partial substitution of 1,4-BG with PCL/clay are given in Table I. In Table I, the number-averaged molecular weight (M_n) of the synthesized PU/clay nanocomposites decreased as the amount of PCL/clay content increased. This can be attributed to the fact that the molecular weight of PCL/clay is 3620 and the concentration of the reactive hydroxy end group of PCL/

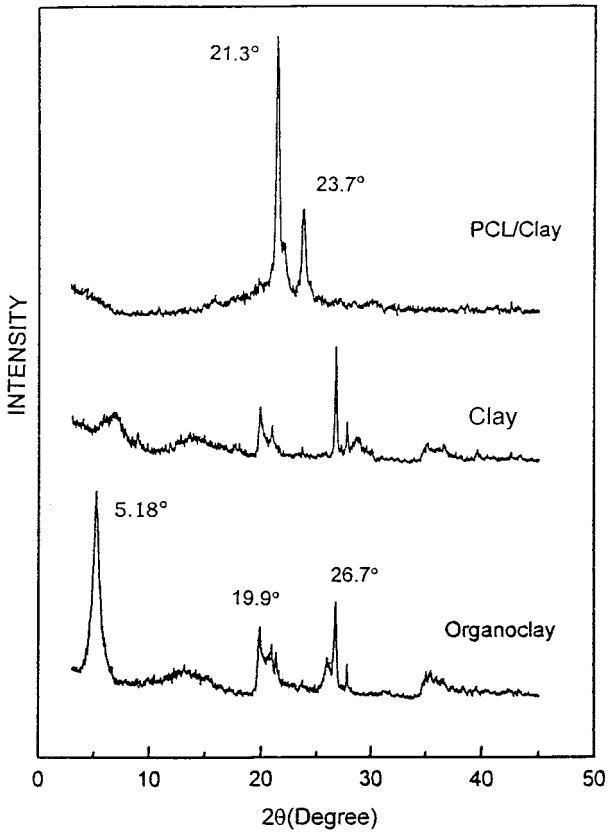

Figure 3. XRD patterns for PCL/5 wt % $[H_3N(CH_2)_{11}COOH]^+$–Mont (PCL/clay), montmorillonite (Na–Mont), and $[H_3N(CH_2)_{11}COOH]^+$–Mont (organoclay).

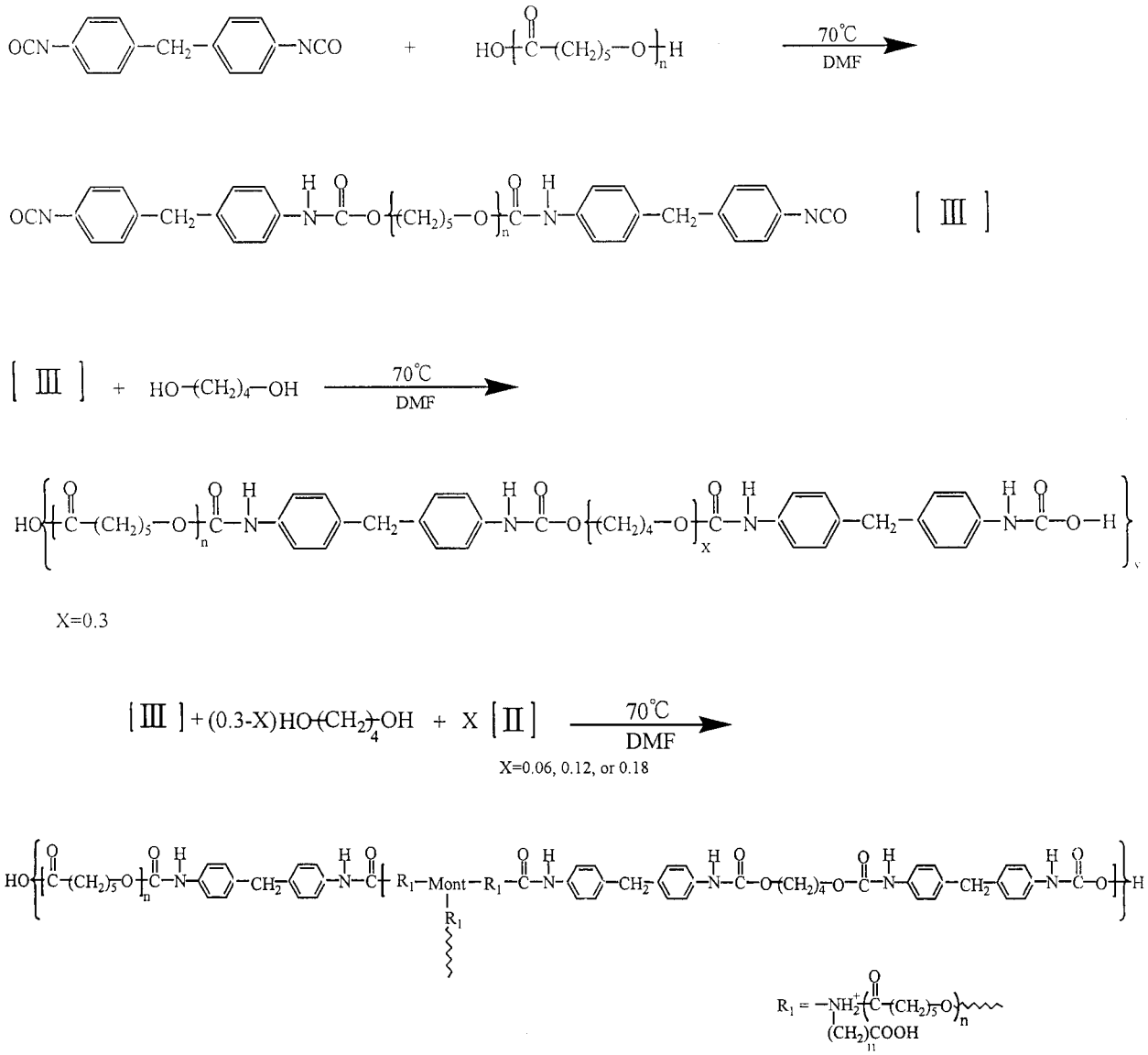

Figure 4. Synthesis of segmented polyurethane/clay, (a) neat PU, (b) PU/clay.

clay is much lower than that of 1,4-BG because of the size of PCL. When the amount of 1,4-BG was replaced by PCL/clay, the molecular weight of synthesized PU decreased after the polymer recovery process, possibly due to the formation of microgel of PCL/clay containing a branch structure to lower gradually the resulting molecular weight of the recovered PU.

The FTIR spectra of these synthesized PU/clay and the neat PU are shown in Figure 5. There are four characteristic absorbance peaks in the spectra of PU20, PU21, PU22, and PU23 to be chosen. The 1710-cm^{-1} peak was caused by the stretching of urethane carbonyl group (C═O), and the 2940 and 2860 cm^{-1} peaks were due to the asymmetric and symmetric C—H stretching vibration. The 3320-cm^{-1} peak resulted from the N—H group in hydrogen bonding. Although absorbance peaks owing to the stretching of the N—H and C—H bonds became sharper for PU23 as compared to that of PU20, the main features of various bond vibration and hydrogen bonding of these PU/clay nanocomposites remained the same as that of neat PU. This result led to the conclusion that there were no major chemical structural changes in PU, owing to the presence of a small amount of PCL/clay. However, the NMR peaks of PU/clay nanocomposites became broadened as the content

Table I. Compositions and Properties of Segmented PU/Clay

	Composition (molar ratio)[a]	PCL/Clay Content (mol %)	Clay Content (wt %)	T_g (°C)	M_n (by GPC)	ΔH (J/g)
PU20	0/1.7/2.2/0.3	0	—	−27.0	52,400	0
PU21	0.06/1.7/2.2/0.24	1.4	0.74	−31.8	31,040[b]	13.6
PU22	0.12/1.7/2.2/0.18	2.8	1.30	−32.0	28,770[b]	27.5
PU23	0.18/1.7/2.2/0.12	4.2	1.70	−32.0	13,810[b]	38.0

[a] Ratio is (PCL/clay)/CAPA214/MDI/1,4-BG.
[b] GPC was performed on polymer recovered from PU/clay nanocomposite using ion exchange reaction.

of PCL/clay increased, as displayed in Figure 6. Since the NMR measurements were carried out in the solution state, this behavior implied that the mobility of the PU molecules in chloroform was restricted by the silicate layers of the clay. The XRD patterns of the synthesized PU/clay nanocomposites are shown in Figure 7. In Figure 7, the XRD patterns of PU21, PU22, and PU23 did not contain any peak at $2\theta = 5.18°$, indicating that these PU/clays are indeed nanocomposites. Moreover, both the intensity and the area of crystalline peak at $2\theta = 21.3°$ and 23.4° increased with the amount of PCL/clay. This resulted from the PCL/clay component in PU/clay by comparing their relative peak positions in Figures 3 and 7.

The DSC curves of the PU/clay are shown in Figure 8. In Figure 8, the T_g of neat PU (PU20) is −27°C, and the T_g of PU/clay nanocomposites is

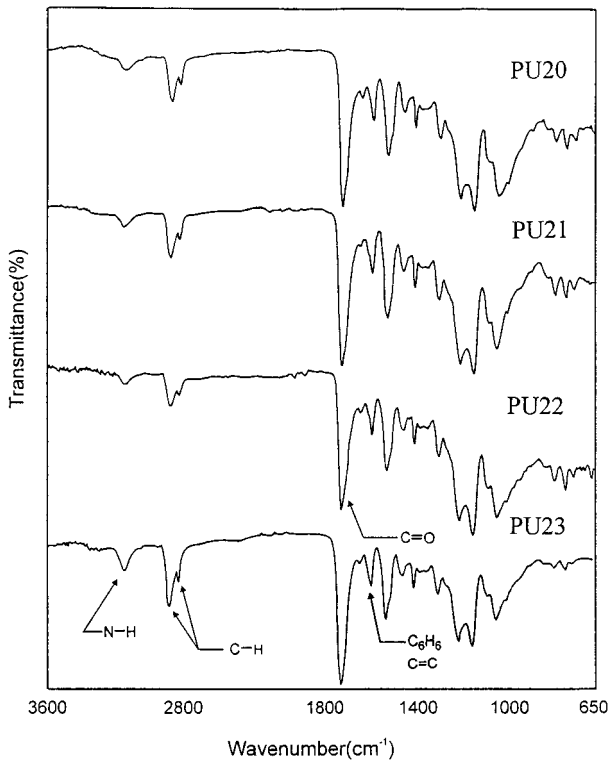

Figure 5. FTIR spectra of segmented polyurethane/clay.

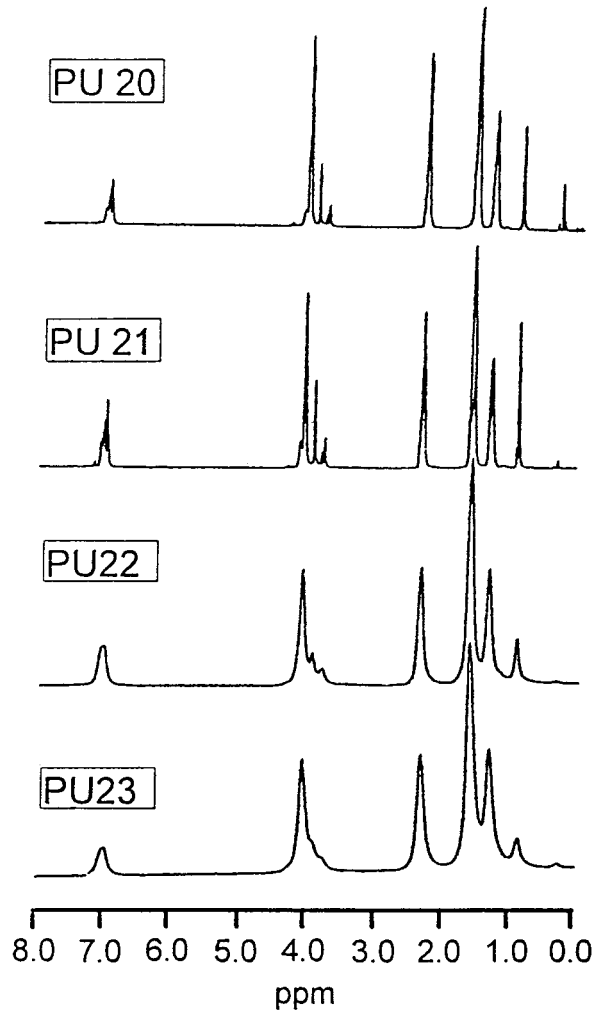

Figure 6. ^{1}H-NMR spectra of segmented polyurethane/clay.

−32°C. The lowering of T_g in PU/clay is due to the increased PCL that was attributed to a partial replacement of 1,4-BG by the PCL/clay. For PU21, there is an endothermic peak at 45°C, and this enthalpy changes because the fusion (ΔH) was 13.6 J/g. The ΔH of PU22 was 27.5 J/g, and it was twice of that of PU21. There seemed to be two endothermic peaks at 45 and 52°C for PU23, and the total ΔH was 38 J/g. The heat of fusion for PU21, PU22, and PU23 are about 28, 49, and 57%, respectively, larger than the values calculated based on the mixing rule from each component. This interesting trend might be explained by the fact that PCL/clay is crystalline, and the dispersed silicate layers in PCL/clay served as nucleation seeds that might have induced some additional crystallinity in the PCL soft segment.

The tensile mechanical properties of PU20, PU21, PU22, and PU23 are given in Table II. In Table II, the tensile strength of segmented PU/clay nanocomposites increased with the amount of PCL/clay. Specifically, the maximum increase in tensile strength is in the case of PU23, where the tensile strength of PU23 is six times that of PU20 (neat PU). This behavior can be attributed to the high tensile strength of the silicate layers of clay dispersed in PU23. However, the elongation behavior of PU/clay nanocomposite is more complex. For the elongation, as listed in Table II, PU21 (containing 1.4% PCL/clay) had a value of 690%, which is 5.7 times that of PU20. The elongation of the PU23 (containing 4.2% PCL/clay) is only 3%. These behaviors can be explained in terms of the structures of PU/clay and the relative amounts of clay and PCL. The segmented PU/clay is based on a partial substitution of 1,4-BG/MDI by (PCL/clay)/MDI in the hard segment. When a small amount of PCL/clay was introduced to PU, the elongation of PU/clay was greatly enhanced because the PCL in PCL/clay can form serial linkage with the original PCL in the soft segment. However, when the amount of PCL/clay is over 3%, the PCL segment in synthesized PCL/clay induced the crystallinity of PCL originally in the soft segment, resulting in an increase in the hard segment domain size and a decrease in the soft segment domain region. Therefore, the elongation of PU23 reduced dramatically. The shear modulus and the lap shear stress of PU/clay are also given in Table II. In Table II, the shear modulus of PU/clay increases dramatically with the amount of PCL/clay. For example, the shear mod-

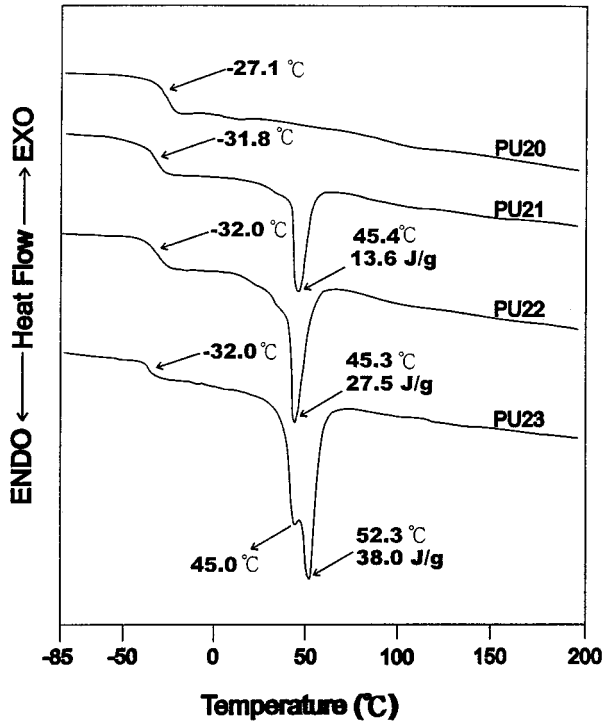

Figure 8. DSC curves of segmented polyurethane/clay.

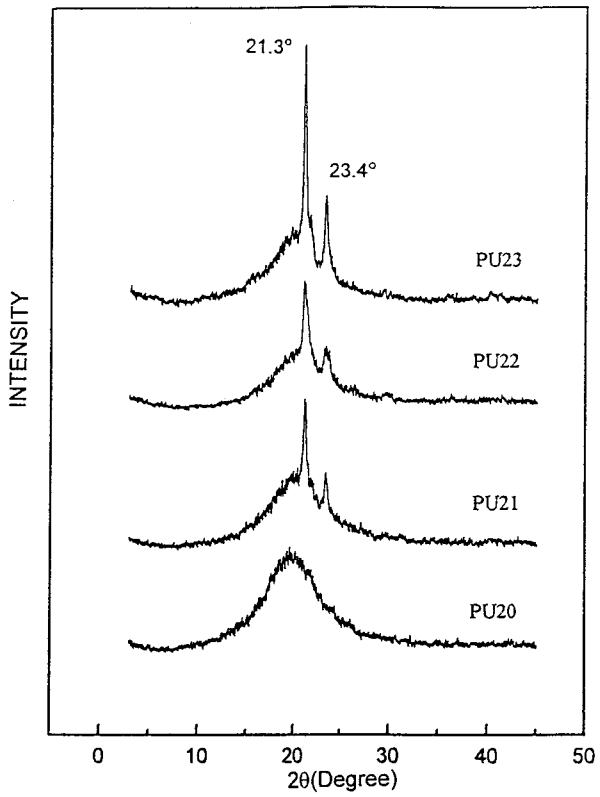

Figure 7. XRD patterns of segmented polyurethane/clay.

Table II. Tensile and Lap Mechanical Properties of Segmented PU/Clay

	Tensile Strength (mPa)	Tensile Elongation (%)	Lap Strength (mPa)	Lap Modulus (mPa)
PU20	0.27	103	0.53	171.0
PU21	0.93	690	1.75	753.0
PU22	1.34	57.5	2.98	1246.0
PU23	1.69	3.3	1.53	1599.0

ulus of PU23 is nine times that of PU20, whereas the lap shear stress of PU22 reached a maximum value of 2.98 mPa, being four times that of PU20. An initial increase in lap shear stress of PU21 and PU22 can be attributed to an increase in cohesion of segmented PU/clay by a partial substitution of 1,4-BG by PCL/clay. However, a further increase in the amount of PCL/clay resulted in an increase in the brittleness of PU/clay, and consequently, reduced the adhesion.

From the tensile strength and the elongation of PU20, PU21, PU22, and PU23, we speculated that the microstructure of PU/clay changed dramatically as the amount of PCL/clay in PU/clay increased. When the amount of PCL/clay is close to 1.4%, most of the silicate layers of PCL/clay are distributed in the hard domain and had little effect on the elongation behavior of PU/clay. The elongation of PU/clay at this stage was dominated by the serial linkage of PCL in the soft segment and in PCL/clay. However, the elongation of PU/clay reduced dramatically when the amount of PCL/clay was close to 4.2%. At this composition, the silicate layers of PCL/clay tended to be dispersed in both the hard and the soft domain, where the hard domain size increased at the expense of the soft domain because of the induced crystallinity of PCL. Therefore, we can have a plausible explanation of the behavior of PU/clay, which can be transformed from an elastomer to a thermoplastic material as the amount of PCL/clay increased.

CONCLUSION

A novel segment PU/clay nanocomposite was synthesized through a partial substitution of PCL/clay for 1,4-BG/MDI. The PCL/clay prepolymer was first synthesized in a nanocomposite form. It was found that the crystallinity and the tensile mechanical properties of these PU/clay nanocomposites were strongly affected by the amount of PCL/clay. The XRD study showed that the PU/clay contained crystalline structures induced by PCL/clay. In mechanical properties, about 1.4% of PCL/clay in PU/clay resulted in a large increase in the elongation of PU/clay. However, when the amount of PCL/clay is 4.2%, the elongation of PU/clay reduced drastically. This behavior indicated that PU/clay can be transformed from an elastomer to a thermoplastic material as the amount of PCL/clay in PU/clay increased. Additionally, the lap shear stress of PU/clay was at least three times that of neat PU as a result of the PCL/clay component.

T. K. Chen thanks the Tze-Chiang Foundation of Science and Technology for providing the research opportunity at the National Chiao Tung University. We also are greatly indebted to Dr. L. H. Perng of Ta Hwa Institute of Technology for helping with the experimental work.

REFERENCES AND NOTES

1. Lam, T. M.; Pascault, J. P. Macromolecules 1992, 25, 5742.
2. Yang, Y. W. D. Mater Lett 1992, 13, 261.
3. Morikawa, A.; Iyoku, Y.; Kakimoio, M. A. Polym J 1992, 24, 689.
4. Long, T. E.; Kelts, L. W. Macromolecules 1991, 24, 1431.
5. Brennan, A. B.; Milleer, T. M. Chem Mater 1994, 6, 262.
6. Wei, Y.; Wang, W.; Yeh, J. M. Polym Prepr 1995, 34, 272.
7. Fujita, M.; Honda, K. Polym Commun 1989, 30, 200.
8. Loy, D. A.; Shea, J. Chem Rev 1995, 95, 1431.
9. Akelah, A.; Moet, A. J Appl Polym Sci: Appl Polym Symp 1994, 55, 153.
10. Kawasumi, M.; Hasegawa, N.; Kato, M.; Usuki, A.; Okada, A. Macromolecules 1997, 30, 6333.
11. Vaia, R. A.; Jandt, K. D.; Kramer, E. J.; Giannelis, E. P. Macromolecules 1995, 28, 8080.

12. Krishnamoorti, R.; Vaia, R. A.; Giannelis, E. P. Chem Mater 1996, 8, 1728.
13. Usuki, A.; Kawasumi, M.; Kojima, Y.; Okada, A.; Kurauchi, T.; Kamigaito, O. J Mater Res 1993, 8, 1174.
14. Usuki, A.; Kojima, Y.; Kawasumi, M.; Okada, A.; Fukushima, Y.; Kurauchi, T.; Kamigaito, O. J Mater Res 1993, 8, 1179.
15. Kojima, Y.; Usuki, A.; Kawasumi, M.; Okada, A.; Kurauchi, T.; Kamigaito, O. J Polym Sci, Polym Chem Ed 1993, 31, 1755.
16. Wang, M. S.; Pinnavaia, T. J. Chem Mater 1994, 6, 468.
17. Messersmith, P. B.; Giannelis, E. P. Chem Mater 1994, 6, 1719.
18. Lan, T.; Kaviratna, P. D.; Pinnavaia, T. J. Chem Mater 1995, 7, 2144.
19. Yano, K.; Usuki, A.; Okada, A.; Kurauchi, T.; Kamigaito, O. J Polym Sci Polym Chem Ed 1993, 31, 2493.
20. Lan, T.; Kaviratna, P. D.; Pinnavaia, T. J. Chem Mater 1994, 6, 573.
21. Vaia, R. A.; Vasudevan, S.; Krawiec, W.; Scanlon, L. G.; Giannelis, E. P. Adv Mater 1995, 7, 154.
22. Giannelis, E. P. Adv Mater 1996, 8, 29.
23. Messersmith, P. B.; Giannelis, E. P. J Polym Sci Polym Chem Ed 1995, 33, 1047.
24. Biasci, L.; Aglietto, M.; Ruggeri, G.; Ciardelli, F. Polymer 1994, 35, 3296.
25. Moet, A.; Akelah, A.; Salahuddin, N.; Hiltner, A.; Baer, E. Mater Res Soc Symp Proc 1994, 351, 163.
26. Burnside, S. D.; Giannelis, E. P. Chem Mater 1995, 7, 1597.
27. Kojima, Y.; Fukumori, K.; Usuki, A.; Okada, A.; Kurauchi, T. J Mater Sci Lett 1993, 12, 889.
28. Wang, C. B.; Cooper, S. L. Macromolecules 1983, 16, 775.
29. Li, F.; Hou, J.; Zhu, W.; Zhang, X.; Xu, M.; Luo, X.; Ma, D.; Kim, B. K. J Appl Polym Sci 1996, 62, 631.
30. Li, F.; Zhang, X.; Hou, J.; Xu, M.; Luo, X.; Ma, D.; Kim, B. K. J Appl Polym Sci 1997, 63, 1511.
31. Usuki, A.; Hasegawa, N.; Okada, A.; Kurauchi, T. Kobunshi Ronbunshu 1995, 52, 576.